Crystal Structure of the Electron Carrier Domain of the Reaction Center Cytochrome c_z Subunit from Green Photosynthetic Bacterium *Chlorobium tepidum*

Yu Hirano[1,2], Makoto Higuchi[1], Chihiro Azai[3], Hirozo Oh-oka[3], Kunio Miki[2,*] and Zheng-Yu Wang[1,*]

Affiliations

[1]*Faculty of Science, Ibaraki University, 2-1-1 Bunkyo, Mito 310-8512, Japan*

[2]*Department of Chemistry, Graduate School of Science, Kyoto University, Sakyo-ku, Kyoto 606-8502, Japan*

[3]*Department of Biological Sciences, Graduate School of Science, Osaka University, Toyonaka, Osaka 560-0043, Japan*

*Corresponding authors

Zheng-Yu Wang

phone +81-29-228-8352, fax +81-29-228-8352, e-mail wang@mx.ibaraki.ac.jp

Kunio Miki

phone +81-75-753-4029, fax +81-75-753-4032, e-mail miki@kuchem.kyoto-u.ac.jp

Running title: Crystal structure of cyt c_z from *Chl. tepidum*

Abstract

In green sulfur photosynthetic bacteria, the cytochrome c_z (cyt c_z) subunit in the reaction center complex mediates electron transfer mainly from menaquinole/cytochrome *c* oxidoreductase to the special pair (P840) of the reaction center. The cyt c_z subunit consists of an N-terminal transmembrane domain and a C-terminal soluble domain that binds a single heme group. The periplasmic soluble domain has been proposed to be highly mobile and to fluctuate between oxidoreductase and P840 during photosynthetic electron transfer. We have determined the crystal structure of the oxidized form of the C-terminal functional domain of the cyt c_z subunit (C-cyt c_z) from thermophilic green sulfur bacterium *Chlorobium tepidum* at 1.3 Å resolution. The overall fold of C-cyt c_z consists of four α-helices and is similar to that of class I cytochrome *c* proteins despite the low similarity in their amino acid sequences. The N-terminal structure of C-cyt c_z supports the swinging mechanism previously proposed in relation with electron transfer, and the surface properties provide useful information on possible interaction sites with its electron transfer partners. Several characteristic features are observed for the heme environment: These include orientation of the axial ligands with respect to the heme plane, surface-exposed area of the heme, positions of water molecules, and hydrogen-bond network involving heme propionate groups. These structural features are essential for elucidating the mechanism for regulating the redox state of cyt c_z.

Keywords: green sulfur bacteria, reaction center, cytochrome c_z, heme, axial ligands

Abbreviations: cyt c_z, cytochrome c_z; C-cyt c_z, the C-terminal domain of cytochrome c_z; $E_{m,7}$, midpoint redox potential at pH 7.0; PEG, polyethylene glycol; PS-I, photosystem I; RC; reaction center; SAD, single anomalous dispersion; SEC-MALS, size exclusion chromatography with multi-angle light scattering; SorB, the heme binding subunit of sulfite-oxidizing molybdoenzyme

Introduction

In photosynthetic organisms such as purple bacteria, cyanobacteria, algae and higher plants, soluble electron carrier proteins are involved in electron transfer between menaquinol/cytochrome *c* oxidoreductase (cytochrome bc_1 complex) or ubiquinol/plastocyanin oxidoreductase (cytochrome b_6f complex) and the reaction center (RC). Different from these organisms, green sulfur bacteria utilize a membrane-anchored cytochrome subunit [cytochrome c_{551}, which has also been named as cytochrome c_z (cyt c_z)] in the RC complex for the corresponding electron transfer. Although membrane-anchored cytochromes in some purple bacteria (cytochrome c_y) and in heliobacteria (cytochrome c_{553}) also mediate such electron transfer,[1,2] these cytochromes have very low similarity in their amino acid sequences and have different arrangements in the membrane-anchoring domain. Cyt c_z has three membrane-spanning regions, whereas cytochrome c_y is anchored by a single membrane-spanning domain, and cytochrome c_{553} is through a fatty acid chain attached to its N-terminus. With respect to the structural diversity in membrane-anchored cytochromes, the evolutionary relationships between these cytochromes have been unclear.

Green sulfur bacteria, which live in a strict anaerobic environment, have a photosynthetic apparatus different from other photosynthetic organisms.[3,4] A large antenna system, called chlorosome, is located at the cytoplasmic side and transfers light energy to the RC. Components of the isolated RC from green sulfur bacteria *Chlorobium limicola* (syn. *Chlorobaculum thiosulfatiphilum*),[5,6] *Chlorobium tepidum* (syn. *Chlorobaculum tepidum*),[6,7] or *Chlorobiumm vibrioforme* (syn. *Chlorobaculum*

parvum)[8] have been reported to consist of five subunits: PscA-PscD and the Fenna-Mathews-Olson protein. The core of the RC is constituted by a homodimer of PscA, which contains the special pair P840. A bacteriochlorophyll A_0 and a quinone A_1 bind to each PscA monomer, and a single Fe-S cluster F_X is chelated to the homodimer. PscB, located at the cytoplasmic side of the PscA dimer, contains two Fe-S clusters (F_A/F_B). A monoheme cytochrome *c*, PscC (cyt c_z), consists of an N-terminal transmembrane domain and a C-terminal periplasmic domain in which a single heme group is bound. This protein is considered as the only electron donor for providing electrons to P840.[9,10] Similar to class I cytochrome proteins, the C-terminal functional domain of cyt c_z (C-cyt c_z) possesses a CXXCH motif with a sixth ligand of methionine. Both PscD and the Fenna-Mathews-Olson protein locate at the cytoplasmic side, and their roles are possibly relevant to energy transfer from chlorosome to the RC.[11]

The RC of green sulfur bacteria possesses an Fe-S cluster as the terminal electron acceptor, and it is thus classified into type I RC along with those of photosystem I (PS-I) from cyanobacteria, algae and higher plants. However, the latter is different from the former especially in that it forms a heterodimeric core consisting of two polypeptides PsaA and PsaB.[12,13] PscA of the green sulfur bacterial RC has been suggested to possess 11 transmembrane helices similar to PsaA/PsaB of the PS-I RC but has weak sequence identities to them. Based on the similarities between PscA and PsaA/PsaB, both RCs have been supposed to evolve from a common ancestor.[12] However, the PS-I RC does not possess a *c*-type cytochrome subunit such as PscC in green sulfur bacteria.

The stoichiometry of cyt c_z has been reported to be one to two molecules per RC depending on preparations.[7,14-17] Flash-induced absorption spectroscopy demonstrated that two copies of cyt c_z bind to one RC in the stable RC complex isolated from *C. tepidum* membrane, and each of them mediates the direct electron transfer mainly from membrane-bound menaquinole/cytochrome *c* oxidoreductase to P840.[18] Because the electron transfer exhibited strong viscosity dependence, the heme binding domain of cyt c_z has been proposed to fluctuate between menaquinole/cytochrome *c* oxidoreductase and P840.[19] Recently, soluble cytochrome c_{554} from *C. tepidum* has been reported to transfer electrons to P840 via cyt c_z.[20] The pathway that confers electrons to cytochrome c_{554} is probably related to thiosulfate oxidation.[21]

Due to the extremely unstable nature of the green sulfur bacterial RC complex under aerobic conditions, its structural information has been largely limited as a result of difficulty in obtaining large quantities of the functionally active preparation. We have developed a system for overexpressing the C-terminal functional domain of cytochrome c_z (C-cyt c_z) from thermophilic *C. tepidum*.[22] In this study, we report the crystal structure of C-cyt c_z and discuss structural features in relation with its functionality. The high-resolution structure provides crucial information for elucidating the molecular mechanism of electron transfer in the photosynthesis of green sulfur bacteria. The structural information is also useful in exploring the evolutionary relationships between cytochrome proteins involved in photosynthetic electron transfer.

Results

Biochemical analyses of the functional domain of cyt c_z

The amino acid sequence of cyt c_z from *C. tepidum* indicates that residues 1-100 constitute three membrane-spanning helices and that residues 110-206 form a soluble domain that contains a CXXCH heme binding motif. For structural analyses of the functional domain of cyt c_z from *C. tepidum*, we constructed a plasmid for expressing the C-terminal domain of cytochrome c_z in *Escherichia coli*.[22] The expression product consists of 90 residues from 117 to 206 and contains the heme *c* binding region. C-cyt c_z was overproduced and the purified C-cyt c_z shows a Soret band at 409 nm in absorption spectrum for the oxidized form. The reduced form by DTT has the Soret band, α-band and β-band at 415, 550.5, and 522 nm, respectively. Equilibrium redox titration of C-cyt c_z showed a midpoint redox potential at pH 7.0 ($E_{m,7}$) of 188±1 mV by fitting with the one-component Nernst equation (Fig. 1a). Oligomeric states of C-cyt c_z in solution were analyzed by size-exclusion chromatography with multi-angle light scattering (SEC-MALS) (Fig. 1b). The purified C-cyt c_z was eluted as a single peak from the column, and the weight average mass was calculated to be 11,600 Da. The result indicates that C-cyt c_z was expressed in monomeric form.

Structure determination of C-cyt c_z

Crystals of oxidized C-cyt c_z were obtained using ammonium sulfate as a precipitant.[22] With the use of polyethylene glycols (PEGs) having a low molecular

weight (PEG200 or PEG400) as an additive, the crystals appeared in a shorter incubation period and the sizes became larger than those without the additive. The crystals belong to space group $I4_1$ with unit cell parameters $a = b = 74.6$, and $c = 111.2$ Å, and the Matthew's coefficient was calculated to be 3.3 Å^3/Da with two molecules in the asymmetric unit. The crystal structure of C-cyt c_z was determined by the single anomalous dispersion (SAD) method using anomalous signals from the heme iron. The final model includes 78 (Thr129-Phe206) and 77 (Ser130-Phe206) residues in chains A and B, respectively, with a working *R* factor of 13.9% and a free *R* factor of 15.5% (Fig. 2a). Double conformations were observed in five amino acid residues (Arg181 in chain A; Lys145, Arg166, Lys180, and His203 in chain B) and in the ring III propionate of the chain A heme. The statistics for data collection, phasing, and refinement are given in Table 1.

Overall structure of C-cyt c_z

C-cyt c_z consists of four α-helices α1 (141-151), α2 (159-168), α3 (175-184), and α4 (192-205) (Fig. 2a). Twelve and 13 residues at the N-termini of chains A and B, respectively, were disordered because the corresponding electron density was not observed, and thus the N-termini of the final model start from Thr129 and Ser130 in chains A and B, respectively. The following 13 and 12 N-terminal residues in chains A and B do not form any secondary structures. 77 C^α atoms of the two chains are superposed with a root-mean-square distance of 0.67 Å. The heme *c* binding motif, C152-XXCH156, is located in the loop between α1 and α2, and the sixth ligand,

Met182, is located at α3 (Fig. 2b). The heme groups covalently bind to the polypeptide chains through thioether linkages of two cysteine residues, Cys152 and Cys155.

Chains A and B face each other at the α1 helices (Fig. 2a). The contact surface area between the two chains is approximately 620 Å^2, corresponding to 6.6% of the total surface area. Their interface features are largely hydrophobic, and three salt bridges are formed between weakly conserved residues, Asp149^A-Lys146^B, Arg151^A-Asp194^B, and Asp194^A-Arg151^B. The heme groups are located at the distal sides from the interface with an iron-iron distance of 31.1 Å (Fig. 2a). Except for the contact in the asymmetric unit, chains A and B contact four and five molecules that surround each chain, respectively. The largest contact surface area is formed between chain A and chain B* (a symmetry-related molecule to chain B) with an approximate buried surface area of 640 Å^2 (Fig. 2c). PEG molecules were observed at the interface between chains A and B*, and the heme groups are located at the same side of the interface with an iron-iron distance of 12.9 Å (Fig. 2d). Other contact surface areas between two neighboring molecules are smaller than 620 Å^2 and inter-iron distances of their heme groups are longer than 31.1 Å.

Structural similarities to other cytochrome *c* proteins

Search of three-dimensional structural homology to C-cyt c_z using the DALI server[23] revealed that the heme binding subunit of sulfite-oxidizing molybdoenzyme (SorB) from the Gram-negative sulfur bacterium *Starkeya novella*[24] has the best

similarity with a *Z*-score of 7.7. It also has structural similarities to cytochrome c_{551} from the Gram-negative bacterium *Pseudomonas aeruginosa*[25] (*Z*-score of 4.5) and to cytochrome c_6 from the green alga *Monoraphidium braunii*[26] (*Z*-score of 4.0). However, the amino acid sequence of C-cyt c_z shows low homology to those of SorB and the two cytochromes (Fig. 3). Only the coordinating residues to their heme groups are completely conserved, and hydrophobic and acidic residues at their C-terminal α-helices are weakly conserved. When protein moieties were superposed between C-cyt c_z and SorB from *S. novella*, both secondary structures and heme groups fit well to each other and the axial ligands have the same orientation (Fig. 4). In contrast, when the secondary structures of C-cyt c_z were superposed on those of cytochrome c_{551} or c_6, the heme group of C-cyt c_z showed large deviation from that of either cytochrome c_{551} or c_6 (data not shown). The heme coordinating residues are also located at different positions between C-cyt c_z and cytochrome c_{551} or c_6. The positional differences of the heme coordinating residues are mainly caused by the shorter loop length in C-cyt c_z between helices α1 and α2 and helices α3 and α4 compared with cytochrome c_{551} or c_6. Inevitably, the secondary structures of C-cyt c_z exhibit large deviation from that of either cytochrome c_{551} or c_6 when the tetrapyrrole ring of C-cyt c_z was superposed on that of cytochrome c_{551} or c_6 (Fig. 5a and c). In the superposition, the heme coordinating residues are located at close positions, while the heme axial ligands (His and Met) of C-cyt c_z show an orientation different from those of cytochrome c_{551} and cytochrome c_6 (Fig. 5b and d). The angle between the imidazole plane of C-cyt c_z His156 and that of cytochrome c_{551} His16 (or c_6 His19) is 86.4º (91.9º), and the angle of

C-cyt c_z Met182 C^{γ}- C-cyt c_z Met182 S^{δ}- cytochrome c_{551} Met61 C^{γ} (or c_6 Met61 C^{γ}) is 100.8º (87.2º).

Heme environment

His156 and Met182 are the axial ligands to the heme iron, and the sulfur atom of the methionine shows *R* stereochemistry. Distances from the heme iron to $N^{\varepsilon 2}$ of His156 and to S^{δ} of Met182 in chain A are (the parenthetical data denote the values of chain B hereinafter) 2.01 Å (2.04 Å) and 2.30 Å (2.32 Å), respectively, and the angle of His156 $N^{\varepsilon 2}$-Fe-Met182 S^{δ} is 174.9º (174.5º). The $N^{\varepsilon 1}$ atom of His156 forms a hydrogen bond with the carbonyl oxygen of Thr157, but S^{δ} of Met182 does not form any hydrogen bonds with the polypeptide chain.

A water molecule binds to the pocket made by the CXXCH motif and the heme tetrapyrrole ring (Fig. 6a). The water molecule (Wat602 in chain A and Wat603 in chain B) is located within hydrogen-bonding distance to the main-chain atoms of the CXXCH motif, such as amide nitrogen of Cys155 and amide nitrogen and carbonyl oxygen of His156. The shortest distance between the water and the constituent atom of the tetrapyrrole ring (carbon 6) is 3.28 Å (3.25 Å), and the distance from the water to the heme iron is 4.76 Å (4.71 Å). SorB from *S. novella* has a water molecule at the same position, but no corresponding water molecule is observed in class I cytochromes, including cytochrome c_{551} and cytochrome c_6. Besides the binding pocket above the heme plane, two water molecules (Wat642 and Wat804) are present in the proximity of the heme propionate of chain A. These water molecules are located at close positions

to the water binding site observed in class I cytochromes, such as yeast mitochondrial cytochrome *c*,[27,28] cytochrome c_2 from the purple bacterium *Blastochloris* (formerly *Rhodopseudomonas*) *viridis*,[29] and cytochrome c_6 from the green alga *Scenedesmus obliquus*.[30] In chain A of C-cyt c_z, a hydrogen bond between the water (Wat804) and Tyr169 has similarities to the hydrogen bond between Wat166 and Tyr67 in yeast mitochondrial cytochrome *c* (Fig. 6b). But unlike the hydrogen bond formed between Tyr67 and the axial ligand Met80 in mitochondrial cytochrome *c*, Tyr169 is too distant to form a hydrogen bond with the axial ligand Met182. In chain B, on the other hand, there are no water molecules near the heme propionates.

The propionates of the heme groups have different conformations between chains A and B, and hydrogen bonds involving the propionates reveal large differences (Fig. 6c). Lys168 in chain A forms a hydrogen bond with the pyrrole ring IV propionate, and Arg181 in chain B does with the pyrrole ring III propionate. Arg181 in chain A forms a hydrogen-bond network consisting of the pyrrole ring III propionate, the two water molecules and the side-chain hydroxyl group of Tyr169. However, Lys168 in chain B does not form any hydrogen bonds to the heme propionates but instead forms a salt bridge to Asp193 of a symmetry-related molecule in the crystal. Crystal packing causes the structural differences of the heme propionates between the two chains as shown in Fig. 2d. The heme propionates of chain A are exposed to the solvent and are therefore readily accessible to water molecules (Fig. 6c). But the heme propionates of chain B are pointed toward the contacting interface with a neighboring molecule. As a result of the contact, conformation of the heme propionates in chain B

is fixed and water molecules are excluded from the vicinity of the heme propionates. In addition, the crystal packing causes a movement of the α2 helix apart from the heme group, making Lys168 and Tyr169 unable to form hydrogen bonds with the heme propionates.

Surface properties

The heme group is largely exposed to the surface of C-cyt c_z at the side of pyrrole rings II and III and both propionates (Fig. 7a). A similar feature was observed for the heme group of SorB from *S. novella*.[24] The exposed region in SorB is located at interface to the molybdenum binding subunit (SorA), and the pyrrole ring III propionate protrudes to the solvent and the substrate-accessible channel between SorA and SorB subunits. In contrast, heme groups of other bacterial monoheme cytochromes are embedded into the hydrophobic interior and less exposed to the surface due to long loops connecting helices I and II and helices III and IV (Fig. 7b).

Kinetic and mutagenetic studies have revealed that a hydrophobic surface area and an electrically charged surface area around the surface-exposed pyrrole ring II edge of cytochrome c_6 are important for electron transfer to the PS-I RC.[31] NMR analyses have also shown that the same region of cytochrome c_6 is involved in the interaction with PS-I[32] or cytochrome *f*.[33] The corresponding surface of C-cyt c_z has a hydrophobic patch (Fig. 7c), and hydrophobic residues (Phe185, Pro186, and Gly187) are located in the vicinity of the surface-exposed pyrrole ring II edge (Fig. 7d). Basic (Arg151, Lys154, Lys180, and Arg181) and acidic (Asp192, Asp193, and Asp194)

residues are flanking the hydrophobic patch. Those hydrophobic and hydrophilic properties are conserved in cyt c_z homologues of green sulfur bacteria (Figure 3).

Discussion

Structural integrity of C-cyt c_z

Both spectroscopic and midpoint potential measurements revealed that the *E.coli*-expressed C-cyt c_z has properties very similar to those of cyt c_z in the purified RC and in the native membrane.[17,18,22] Subtle differences might be due to the presence of detergents, lipids, or other RC subunits in the purified RC or in the native membrane, and the discrepancies are the same range as observed for the soluble variant of membrane-anchored cytochrome c_y.[34] These spectroscopic and electrochemical analyses indicate that the recombinant C-cyt c_z has the same protein fold and heme group coordination as in the native cyt c_z.

Possible interaction manner with the physiological electron transfer partners

Every buried surface area between two neighboring chains in the crystal is less than 640 Å^2 which is quite smaller than the average value of typical protein-protein complexes.[35] In addition, the molecular weight of C-cyt c_z analyzed by SEC-MALS indicates that it exists as a monomer in solution. Therefore, each periplasmic domain of the two cyt c_z subunits may act as a monomer in the RC complex. It agrees with the electron transfer model that two cyt c_z's appeared to behave independently as an electron donor to P840.[36] However, the edge-to-edge distance between the heme of chain A and that of chain B* is within the typical electron tunneling distance (Fig. 2d).[37] This complex might indicate an arrangement for the interaction between one of the two periplasmic domains of cyt c_z and soluble cytochrome c_{554}.[20] It is also possible that the

periplasmic domains transiently form the complex as observed between electron transfer partners.[38] The N-termini of chains A and B* are located at the same side of the molecules (Fig. 2c). This arrangement indicates that the transmembrane regions are linked to the same direction of the two chains and is thus favorable for the interaction between the periplasmic domains. On the other hand, the possibility that the crystallization condition could induce formation of the complex remains. Crystals of C-cyt c_z grew large and appeared in a short incubation period only when the crystallization solution contained PEG. PEG molecules may promote crystal growth by binding to the hydrophobic clefts to prevent the two chains from unspecific interactions and therefore to fix the positions of the two chains (Fig. 2d).

Although interaction manners between cyt c_z and its electron transfer partners have not been elucidated, those between cytochrome c_6 and PS-I or cytochrome *f* have been well studied.[26,31-33] These studies have shown that the hydrophobic patch near the surface-exposed pyrrole ring II edge is important for electron transfer reaction and that the hydrophilic area around the patch is responsible for complex formation. C-cyt c_z has similar properties at the corresponding surface (Fig. 7c and d). In addition, the heme pyrrole ring II of cytochrome c_2 locates at the closest distance from the special pair of the RC in the crystal structure of the purple bacterial cytochrome c_2-RC complex,[39] and the heme pyrrole ring II of cytochrome *c* does from the heme c_1 of the cytochrome bc_1 complex in the crystal structure of the mitochondrial cytochrome *c*-bc_1 complex.[40] Those results of the electron transfer complexes suggest that the region around the surface-exposed pyrrole ring II edge is also a possible binding site of cyt c_z

to electron transfer partners. Further structural information on the RC and menaquinole/cytochrome *c* oxidoreductase of green sulfur bacteria is required to explore the interactions between the electron transfer proteins.

The N-terminal residues from Ala117-Ala127 of C-cyt c_z are disordered in the crystal structure, and the following 13 residues (Ala128-Asp140) form a loop structure. These residues correspond to an inter-domain linker between the transmembrane and the periplasmic domains of cyt c_z. Thus, the structural features reflect a flexibility of the inter-domain linker of cyt c_z. High alanine and proline contents within the region also suggest that at least 15 residues (Pro126-Asp140) form a flexible structure (the gray box in Fig. 3). The length of inter-domain linker formed by less than 40 residues in cyt c_z is shorter than that of cytochrome c_y.[41] The short linker implies that cyt c_z locates in close proximity to both the RC and the menaquinole/cytochrome *c* oxidoreductase. Indeed, cyt c_z exists as a subunit in the RC complex and is thought to contact closely with the PscA dimer, while cytochrome c_y is connected with the RC intervened by the light-harvesting complex that surrounds the RC. The inter-domain structure well explains the fluctuating behavior observed for the periplasmic domain of cyt c_z in the electron transfer from menaquinole/cytochrome *c* oxidoreductase to P840.[19]

Adjustment of heme redox state

C-cyt c_z possesses structural homologies to two cytochrome proteins (cytochrome c_{551} and cytochrome c_6). However, there are three distinct differences in the heme environment. First, the axial ligands display different orientations relative to

the heme plane (Fig. 5). The orientation of the axial ligands could affect the redox state and therefore regulate electron transfer as the axial ligands directly influence the electron distribution of the heme iron. The difference in orientation may relate with an observation of unusually large paramagnetic shifts in the ^{1}H NMR spectrum of the oxidized C-cyt c_z[22] since the axial ligand orientation has been reported to correlate with the ^{1}H NMR shifts of heme proteins.[42,43] Second, a large area of the heme group is exposed to the surface (Fig. 7a). For the cytochrome subunits of purple bacterial RCs, the heme groups exposed to solvent have lower redox potentials than those buried in the hydrophobic interior.[44] The fact that C-cyt c_z has a lower $E_{m,7}$ value (approximately +190 mV) than cytochrome c_{551} (approximately +270 mV)[45] or c_6 (approximately +370 mV)[46] may indicate a high solvent accessibility of the C-cyt c_z heme. Third, a water molecule is bound in the pocket formed by the tetrapyrrole ring and the CXXCH motif (Fig. 6a). The water molecule could influence not only the electron distribution in the tetrapyrrole ring but also the loop structure around the CXXCH motif by modifying hydrogen-bonding pattern. Because conformational mobility of the CXXCH motif was reported to modulate the heme redox potential in *P. aeruginosa* cytochrome c_{551},[45] the water moloecule in the C-cyt c_z heme pocket may also regulate its redox potential.

In addition to the differences mentioned above, C-cyt c_z has characteristic structural features around the heme propionates. Two water molecules near the heme propionates are found at different positions from the water molecule (Wat166) conserved in mitochondrial cytochrome *c* (Fig. 6b).[27] The latter was shown to play a role in maintaining the midpoint redox potential of the heme group. Especially, a

tyrosine residue (Tyr67) was suggested to stabilize the redox state through hydrogen bonds with the water molecule and the axial ligand Met80. On the other hand, in C-cyt c_z, the two water molecules are found only in chain A and Tyr169 forms a hydrogen bond with Wat804 but not with the axial ligand Met182 (Fig. 6c). Thus, the redox stabilization effect by the two water molecules and Tyr169 is probably weaker than Wat166 and Tyr67 in mitochondrial cytochrome *c*. The hydrogen bonds in C-cyt c_z may contribute to lowering the redox potential by neutralizing the propionates as reported for cytochrome c_{6A} (a higher plant counterpart of cytochrome c_6).[46]

Implication for evolutionary relationships between cytochromes

Some purple photosynthetic bacteria possess membrane-anchored cytochromes with a role similar to cyt c_z. Cytochrome c_y from *Rhodobacter capsulatus*[34] and cytochrome *c* from *Rhodovulum sulfidophilum*[47] function as electron transfer mediators from the cytochrome bc_1 complex to the RC. The amino acid sequence of cytochrome c_y from *R. capsulatus* is similar to that of membrane-bound cytochrome c_{552} from *Paracoccus denitrificans*. The soluble domain of cytochrome c_{552} has structural resemblances to mitochondrial cytochrome *c*.[48] The heme binding domain of cytochrome *c* from *R. sulfidophilum* has sequence similarity to purple bacterial cytochrome c_2. In heliobacteria, cytochrome c_{553} transfers electrons from menaquinol/cytochrome *c* oxidoreductase to the RC.[1] The amino acid sequence of cytochrome c_{553} from *Heliobacillus mobilis* is similar to that of cytochrome c_{551} from *P. aeruginosa* (35% identity and 56% similarity over 82 amino acids). As a consequence,

the heme coordination of C-cyt c_z is different from that of membrane-anchored cytochromes c_y, c and c_{553}. Based on the differences in the structure, amino acid sequence and membrane-spanning arrangement, these cytochromes may not have evolved from a common origin or may have diverged in the early stage of evolution. In contrast, notable similarity of the structures between C-cyt c_z and SorB suggests that cyt c_z and SorB have some evolutionary relationship. *C. tepidum* is an anaerobic phototrophic bacterium that utilizes reduced sulfur compounds for carbon dioxide fixation, and *S. novella* is a chemolithotrophic bacterium that utilizes thiosulfate as an energy source. They have common sulfur-oxidizing (sox) proteins,[49,50] and cytochromes from the SoxAX family may be involved in thiosulfate oxidation.[51] Thus, cyt c_z and SorB might have derived from a common origin that had been utilized for sulfur metabolism. The N-terminal long loop in the crystal structure of SorB[24] also shows that the deletion of transmembrane domain might have occurred during the evolution of SorB.

Membrane-bound cytochromes that mediate photosynthetic electron transfer have never been observed in cyanobacteria, algae, or higher plants in which water-soluble electron carriers (cytochrome c_6 or plastocyanin) are alternatively utilized. Restriction of diffusion in membrane-bound cytochromes might be unfavorable to these aerobic organisms for efficient photosynthetic turnover. Nevertheless, cyt c_z functionally resembles cytochrome c_6 that shuttles electrons from the cytochrome b_6f complex to the PS-I RC. Despite the functional similarity, structural features of C-cyt c_z indicate that cytochrome c_6 may not derive from cyt c_z as a result of deletion of the

transmembrane domain. Exposure of the large area of the heme group may suffer from oxidation by oxygen atoms dissolving in growth media or in the air; thus, the strict anaerobic growth condition of green sulfur bacteria enables utilization of cyt c_z for the indispensable electron transfer during photosynthesis. Because of its inherent sensitivity to the surrounding environment, cyt c_z may be replaced with cytochrome c_6 in cyanobacteria or algae.

Materials and Methods

Cloning, expression, and purification

The soluble domain of cyt c_z from *C. tepidum* (residues 117-206, C-cyt c_z) was expressed in *E. coli* C41 cell with *ccm* gene clusters, as previously described.[22] C-cyt c_z was isolated from periplasmic fraction, and the quality of the finally purified sample was assessed by SDS-PAGE and UV-vis absorption spectrum.

Redox titration

Redox titrations were performed as described previously.[17] Measurements were carried out three times under a continuous flow of argon gas for keeping the vessel anaerobic. An ORP electrode and a reference $Ag/AgCl_2$ electrode were used for the titrations of C-cyt c_z in 100 mM potassium phosphate buffer, pH 7.0, containing 10 μM 2,3,5,6-tetramethyl-1,4-phenylenediamine, 10 μM phenazine ethosulfate, 10 μM phenazine methosulfate, and 10 μM 2-methyl-1,4-naphthoquinone as redox mediators. Midpoint potentials were determined from absorption changes of cytochrome α-band at 551 nm against voltage and were fitted to the one-component Nernst equation with a least-squares-fit program.

SEC-MALS

The solution state of the purified C-cyt c_z was analyzed using an analytical SEC with online MALS and UV detection. A Superdex 75 column (GE healthcare) was used for the SEC, and a miniDAWN TREOS (Wyatt Technology) detector was used

for the light scattering. The column was equilibrated with 50 mM Tris-HCl, pH 7.5, and 250 mM sodium chloride. One hundred microliters of C-cyt c_z was loaded on the column at a concentration of 0.8 mg/ml and eluted at a flow rate of 0.5 ml/min. The weight average mass of C-cyt c_z was analyzed with the *Astra V* software (Wyatt Technology). For calculation of the weight average mass, the concentration of C-cyt c_z was determined from the UV absorption profile of SEC. The extinction coefficient at 280 nm was estimated from that at 550-535 nm in a reduced minus oxidized spectrum of C-cyt c_z ($\varepsilon_{R\text{-}O,550\text{-}535}$ = 20.2 mM^{-1} cm^{-1}), which was determined by the concentration of the pyridine hemochrome.[52]

Crystallization

Crystallization conditions of oxidized C-cyt c_z have been reported previously.[22] Initial crystals were appeared 2 months after the crystallization setup, and the sizes of the crystals were very small (less than 0.02 mm in the longest dimension). Additive screening was performed to improve the crystal quality and the sizes, and then crystals grew in 2 weeks with larger sizes (~0.2 mm × 0.1 mm × 0.1 mm) when PEGs of low molecular weights (PEG200 or PEG400) were added.

Data collection and phasing

Prior to data collection, the crystals were transferred into the reservoir solution supplemented with 20% (*v*/*v*) glycerol and then flash-cooled in nitrogen-gas stream at 100K. The Fe-SAD and the highest-resolution data were collected at

beamlines 5A of PF and NW12A of PF-AR (KEK, Tsukuba, Japan), respectively. The wavelength for the Fe-SAD data collection (1.7365 Å) was determined based on the X-ray absorption spectrum.

All data were processed and scaled using the *HKL2000* program package.[53] The SAD data set was indexed and scaled to 2.0-Å resolution, and the redundancies of the whole resolution range and the highest-resolution shell were 22.5 and 9.8, respectively. Two iron sites were clearly observed in the anomalous difference Patterson map, and phase calculation and refinement were performed by *OASIS*.[54] The initial electron density map was improved by solvent flattering using *DM*,[55] and the map calculated in the space group $I4_1$ exhibited clear boundary between molecules and solvent. Automated building of the amino acid chain was performed using *ARP*/*wARP*,[56] and 152 residues can be traced with the initial phase. The positions of two heme groups were clearly observed in the sigmaA-weighted F_o-F_c electron density map calculated from the phases of the initial model. After incorporating two heme groups and modifying the initial model by hand, structure refinement was achieved using the highest resolution data collected to 1.3-Å resolution.

Refinement

We started structure refinement from the initial model using the highest-resolution data collected to 1.3-Å resolution. Five percent of the reflections were set aside as free *R* factor calculation. The initial model from the automated model building was subjected to rigid-body refinement at 8- to 1.3-Å resolution using the

program *CNS*,[57] treating each chain as a rigid group. After the rigid-body refinement, heme groups were incorporated in the model and amino acid residues were manually modified using *Coot*.[58] Several cycles of simulated annealing and *B*-factor refinement with bulk solvent correction were performed at 50- to 1.3-Å resolution. Residues 129-206 and 130-206 were traced and solvent molecules (three PEGs, a sodium ion, a sulfate ion and 269 water molecules) were included in the model (R_{work}= 18.9% and R_{free}= 20.5%). Then, refinement with anisotropic displacement parameters was performed using *Refmac5*.[59] Double conformations were incorporated in five residues and in the heme ring III propionate of chain A, and the final structure was refined to R_{work}= 13.9% and R_{free}= 15.5%.

The quality of the structure was analyzed using *MolProbity*.[60] Figures were prepared with *PyMol*,[61] and the surface potentials were calculated by using the Poisson-Boltzmann equation implemented by the Adaptive Poisson-Boltzmann Solver.[62]

Accession number

The coordinate and structure factor of C-cyt c_z have been deposited in Protein Data Bank under accession number 3A9F.

Reference

1. Oh-oka, H. (2007). Type 1 reaction center of photosynthetic heliobacteria. *Photochem. Photobiol.* **83**, 177-186.
2. Azai, C., Tsukatani, Y., Itoh, S. & Oh-oka, H. (2010) C-type cytochromes in the photosynthetic electron transfer pathways in green sulfur bacteria and heliobacteria. *Photosynth. Res.* in press.
3. Hauska, G., Schoedl, T., Rémigy, H. & Tsiotis, G. (2001). The reaction center of green sulfur bacteria. *Biochim. Biophys. Acta* **1507**, 260-277.
4. Rémigy, H. W., Hauska, G., Müller, S. A. & Tsiotis, G. (2002). The reaction centre from green sulphur bacteria: progress towards structural elucidation. *Photosynth. Res.* **71**, 91-8.
5. Hurt, E. C. & Hauska, G. (1984). Purification of membrane-bound cytochromes and a photoactive P840-protein complex of the green sulfur bacterium *Chlorobium-limicola* f. *thiosulfatophilum*. *FEBS Lett.* **168**, 149-154.
6. Hagar-Braun, C., Xie, D. L., Jarosch, U., Herold, E., Büttner, M., Zimmermann, R., Deutzmann, R., Hauska, G. & Nelson, N. (1995). Stable photobleaching of P840 in *Chlorobium* reaction-center preparations - presence of the 42-kDa bacteriochlorophyll *a* protein and a 17-kDa polypeptide. *Biochemistry* **34**, 9617-9624.
7. Kusumoto, N., Inoue, K., Nasu, H. & Sakurai, H. (1994). Preparation of a photoactive reaction-center complex containing photo-reducible Fe-S centers and photooxidizable cytochrome-c from the green sulfur bacterium *Chlorobium tepidum*. *Plant Cell Physiol.* **35**, 17-25.
8. Kjær, B. & Scheller, H. V. (1996). An isolated reaction center complex from the green sulfur bacterium *Chlorobium vibrioforme* can photoreduce ferredoxin at high rates. *Photosynth. Res.* **47**, 33-39.
9. Oh-oka, H., Iwaki, M. & Itoh, S. (1998). Membrane-bound cytochrome c_z couples quinol oxidoreductase to the P840 reaction center complex in isolated membranes of the green sulfur bacterium *Chlorobium tepidum*. *Biochemistry* **37**, 12293-12300.
10. Tsukatani, Y., Miyamoto, R., Itoh, S. & Oh-oka, H. (2006). Soluble cytochrome

c-554, CycA, is not essential for photosynthetic electron transfer in *Chlorobium tepidum*. *FEBS Lett*. **580**, 2191-2194.

11. Tsukatani, Y., Miyamoto, R., Itoh, S. & Oh-Oka, H. (2004). Function of a PscD subunit in a homodimeric reaction center complex of the photosynthetic green sulfur bacterium *Chlorobium tepidum* studied by insertional gene inactivation. Regulation of energy transfer and ferredoxin-mediated $NADP^+$ reduction on the cytoplasmic side. *J. Biol. Chem.* **279**, 51122-51130.
12. Olson, J. M. & Blankenship, R. E. (2004). Thinking about the evolution of photosynthesis. *Photosynth. Res.* **80**, 373-386.
13. Heathcote, P., Jones, M. R. & Fyfe, P. K. (2003). Type I photosynthetic reaction centres: structure and function. *Philos. Trans. R. Soc. London, Ser. B* **358**, 231-243.
14. Okkels, J. S., Kjær, B., Hansson, Ö., Svendsen, I., Møller, B. L. & Scheller, H. V. (1992). A membrane-bound monoheme cytochrome c_{551} of a novel type is the immediate electron donor to P840 of the *Chlorobium vibrioforme* photosynthetic reaction center complex. *J. Biol. Chem.* **267**, 21139-21145.
15. Feiler, U., Nitschke, W. & Michel, H. (1992). Characterization of an improved reaction center preparation from the photosynthetic green sulfur bacterium *Chlorobium* containing the FeS centers F_A and F_B and a bound cytochrome subunit. *Biochemistry* **31**, 2608-2614.
16. Ohoka, H., Kakutani, S., Matsubara, H., Malkin, R. & Itoh, S. (1993). Isolation of the photoactive reaction center complex that contains 3 types of Fe-S centers and a cytochrome-c subunit from the green sulfur bacterium *Chlorobium limicola* f. *thiosulfatophilum*, strain Larsen. *Plant Cell Physiol*. **34**, 93-101.
17. Okumura, N., Shimada, K. & Matsuura, K. (1994). Photo-oxidation of membrane-bound and soluble cytochrome *c* in the green sulfur bacterium *Chlorobium tepidum*. *Photosynth. Res*. **41**, 125-134.
18. Oh-oka, H., Kamei, S., Matsubara, H., Iwaki, M. & Itoh, S. (1995). Two molecules of cytochrome *c* function as the electron donors to P840 in the reaction center complex isolated from a green sulfur bacterium, *Chlorobium tepidum*. *FEBS Lett*. **365**, 30-34.
19. Oh-oka, H., Iwaki, M. & Itoh, S. (1997). Viscosity dependence of the electron transfer rate from bound cytochrome *c* to P840 in the photosynthetic reaction

center of the green sulfur bacterium *Chlorobium tepidum*. *Biochemistry* **36**, 9267-9272.

20. Tsukatani, Y., Azai, C., Kondo, T., Itoh, S. & Oh-Oka, H. (2008). Parallel electron donation pathways to cytochrome c_z in the type I homodimeric photosynthetic reaction center complex of *Chlorobium tepidum*. *Biochim. Biophys. Acta* **1777**, 1211-1217.
21. Azai, C., Tsukatani, Y., Harada, J. & Oh-oka, H. (2009). Sulfur oxidation in mutants of the photosynthetic green sulfur bacterium *Chlorobium tepidum* devoid of cytochrome *c*-554 and SoxB. *Photosynth. Res.* **100**, 57-65.
22. Higuchi, M., Hirano, Y., Kimura, Y., Oh-Oka, H., Miki, K. & Wang, Z.-Y. (2009). Overexpression, characterization and crystallization of the functional domain of cytochrome c_z from *Chlorobium tepidum*. *Photosynth. Res.* **102**, 77-84.
23. Holm, L. & Sander, C. (1995). Dali - a network tool for protein-structure comparison. *Trends Biochem. Sci.* **20**, 478-480.
24. Kappler, U. & Bailey, S. (2005). Molecular basis of intramolecular electron transfer in sulfite-oxidizing enzymes is revealed by high resolution structure of a heterodimeric complex of the catalytic molybdopterin subunit and a *c*-type cytochrome subunit. *J. Biol. Chem.* **280**, 24999-25007.
25. Matsuura, Y., Takano, T. & Dickerson, R. E. (1982). Structure of cytochrome c_{551} from *Pseudomonas aeruginosa* refined at 1.6 Å resolution and comparison of the two redox forms. *J. Mol. Biol.* **156**, 389-409.
26. Frazão, C., Soares, C. M., Carrondo, M. A., Pohl, E., Dauter, Z., Wilson, K. S., Hervás, M., Navarro, J. A., De la Rosa, M. A. & Sheldrick, G. M. (1995). *Ab initio* determination of the crystal structure of cytochrome c_6 and comparison with plastocyanin. *Structure* **3**, 1159-1169.
27. Berghuis, A. M., Guillemette, J. G., McLendon, G., Sherman, F., Smith, M. & Brayer, G. D. (1994). The role of a conserved internal water molecule and its associated hydrogen bond network in cytochrome *c*. *J. Mol. Biol.* **236**, 786-799.
28. Berghuis, A. M. & Brayer, G. D. (1992). Oxidation state-dependent conformational changes in cytochrome *c*. *J. Mol. Biol.* **223**, 959-976.
29. Sogabe, S. & Miki, K. (1995). Refined crystal structure of ferrocytochrome c_2 from *Rhodopseudomonas viridis* at 1.6 Å resolutinon. *J. Mol. Biol.* **252**, 235-

247.

30. Schnackenberg, J., Than, M. E., Mann, K, Wiegand, G., Huber, R. & Reuter, W. (1999). Amino acid sequence, crystallization and structure determination of reduced and oxidized cytochrome c_6 from the green alga *Scenedesmus obliquus*. *J. Mol. Biol.* **290**, 1019-1030.

31. Díaz-Quintana, A., Navarro, J. A., Hervás, N., Molina-Heredia, F. P., De la Cerda, B. & De la Rosa, M. A. (2003). A comparative structural and functional analysis of cyanobacterial plastocyanin and cytochrome c_6 as alternative electron donors to photosystem I. *Photosynth. Res.* **75**, 97-110.

32. Díaz-Moreno, I., Díaz-Quintana, A., Molina-Heredia, F. P., Nieto, P. M., Hansson, Ö., De la Rosa, M. A., Karlsson, B. G. (2005). NMR analysis of the transient complex between membrane photosystem I and soluble cytochrome c_6. *J. Biol. Chem.* **280**, 7925-7931.

33. Crowley, P. B., Díaz-Quintana, A., Molina-Heredia, F. P., Nieto, P., Sutter, M., Haehnel, W., De la Rosa, M. A., Ubbink, M. (2002). The interactions of cyanobacterial cytochrome c_6 and cytochrome *f*, characterized by NMR. *J. Biol. Chem.* **277**, 48685-48689.

34. Öztürk, Y., Lee, D. W., Mandaci, S., Osyczka, A., Prince, R. C. & Daldal, F. (2008). Soluble variants of *Rhodobacter capsulatus* membrane-anchored cytochrome c_y are efficient photosynthetic electron carriers. *J. Biol. Chem.* **283**, 13964-13972.

35. Lo Conte, L., Chothia, C. & Janin, J. (1999). The atomic structure of protein-protein recognition sites. *J. Mol. Biol.* **285**, 2177-2198.

36. Kusumoto, N., Setif, P., Brettel, K., Seo, D. & Sakurai, H. (1999). Electron transfer kinetics in purified reaction centers from the green sulfur bacterium *Chlorobium tepidum* studied by multiple-flash excitation. *Biochemistry* **38**, 12124-12137.

37. Page, C. C., Moser, C. C. & Dutton, P. L. (2003). Mechanism for electron transfer within and between proteins. *Curr. Opin. Chem. Biol.* **7**, 551-556.

38. Crowley, P. B. & Carrondo, M. A. (2004). The architecture of the binding site in redox protein complexes: implications for fast dissociation. *Proteins* **55**, 603-612.

39. Axelrod, H. L., Abresch, E. C., Okamura, M. Y., Yeh, A. P., Rees, D. C. & Feher,

G. (2002). X-ray structure determination of the cytochrome c_2: reaction center electron transfer complex from *Rhodobacter sphaeroides*. *J. Mol. Biol.* **319**, 501-515.

40. Lange, C. & Hunte, C. (2002). Crystal structure of the yeast cytochrome bc_1 complex with its bound substrate cytochrome *c*. *Proc. Natl. Acad. Sci. USA* **99**, 2800-2805.

41. Lee, D. W., Öztürk, Y., Osyczka, A., Cooley, J. W. & Daldal, F. (2008). Cytochrome bc_1-c_y fusion complexes reveal the distance constraints for functional electron transfer between photosynthesis components. *J. Biol. Chem.* **283**, 13973-13982.

42. Shokhirev, N. V. & Walker, F. A. (1998). The effect of axial ligand plane orientation on the contact and pseudocontact shifts of the low-spin ferriheme proteins. *J. Biol. Inorg. Chem.* **3**, 581-594.

43. Tachiiri, N., Hemmi, H., Takayama, S. J., Mita, H., Hasegawa, J., Sambongi, Y. & Yamamoto, Y. (2004). Effects of axial methionine coordination on the in-plane asymmetry of the heme electronic structure of cytochrome *c*. *J. Biol. Inorg. Chem.* **9**, 733-742.

44. Voigt, P. & Knapp, E. W. (2003). Tuning heme redox potentials in the cytochrome *c* subunit of photosynthetic reaction centers. *J. Biol. Chem.* **278**, 51993-52001.

45. Michel, L. V., Ye, T., Bowman, S. E., Levin, B. D., Hahn, M. A., Russell, B. S., Elliott, S. J. & Bren, K. L. (2007). Heme attachment motif mobility tunes cytochrome *c* redox potential. *Biochemistry* **46**, 11753-11760.

46. Worrall, J. A., Schlarb-Ridley, B. G., Reda, T., Marcaida, M. J., Moorlen, R. J., Wastl, J., Hirst, J., Bendall, D. S., Luisi, B. F. & Howe, C. J. (2007). Modulation of heme redox potential in the cytochrome c_6 family. *J. Am. Chem. Soc.* **129**, 9468-9475.

47. Kimura, Y., Alric, J., Vermeglio, A., Masuda, S., Hagiwara, Y., Matsuura, K., Shimada, K. & Nagashima, K. V. (2007). A new membrane-bound cytochrome *c* works as an electron donor to the photosynthetic reaction center complex in the purple bacterium, *Rhodovulum sulfidophilum*. *J. Biol. Chem.* **282**, 6463-6472.

48. Harrenga, A., Reincke, B., Rüterjans, H., Ludwig, B. & Michel, H. (2000). Structure of the soluble domain of cytochrome c_{552} from *Paracoccus*

denitrificans in the oxidized and reduced states. *J. Mol. Biol.* **295**, 667-678.

49. Friedrich, C. G., Rother, D., Bardischewsky, F., Quentmeier, A. & Fischer, J. (2001). Oxidation of reduced inorganic sulfur compounds by bacteria: emergence of a common mechanism? *Appl. Environ. Microbiol.* **6**, 2873-2882.
50. Friedrich, C. G., Bardischewsky, F., Rother, D., Quentmeier, A. & Fischer, J. (2005). Prokaryotic sulfur oxidation. *Curr. Opin. Microbiol.* **8**, 253-259.
51. Kappler, U., Aguey-Zinsou, K.-F., Hanson, G. R., Bernhardt, P. V., McEwan, A. G. (2004). Cytochrome c_{551} from *Starkeya novella*. *J. Biol. Chem.* **279**, 6252-6260.
52. Berry, E. A. & Trumpower, B. L. (1987). Simultaneous determination of hemes *a*, *b*, and *c* from pyridine hemochrome spectra. *Anal. Biochem.* **161**, 1-15.
53. Otwinowski, Z. & Minor, W. (1997). Processing of X-ray diffraction data collected in oscillation mode. *Methods Enzymol.* **276**, 307-326.
54. Hao, Q., Gu, Y. X., Zheng, C. D. & Fan, H. F. (2000). *OASIS*: a computer program for breaking phase ambiguity in one-wavelength anomalous scattering or single isomorphous substitution (replacement) data. *J. Appl. Crystallogr.* **33**, 980-981.
55. Cowtan, W. (1994). 'dm': An automated procedure for phase improvement by density modification. *Jt. CCP4-ESF-EASCBM Newsl. Prot. Crystallogr.* **31**, 34-38.
56. Perrakis, A., Morris, R. & Lamzin, V. S. (1999). Automated protein model building combined with iterative structure refinement. *Nature Struct. Biol.* **6**, 458-463.
57. Brunger, A. T., Adams, P. D., Clore, G. M., DeLano, W. L., Gros, P., Grosse-Kunstleve, R. W., Jiang, J. S., Kuszewski, J., Nilges, M., Pannu, N. S., Read, R. J., Rice, L. M., Simonson, T. & Warren, G. L. (1998). Crystallography & NMR System: a new software suite for macromolecular structure determination. *Acta Crystallogr., Sect. D: Biol. Crystallogr.* **54**, 905-921.
58. Emsley, P., Lohkamp, B., Scott, W. & Cowtan, K. (in press). Features and development of Coot. *Acta Crystallogr., Sect. D: Biol. Crystallogr.*
59. Murshudov, G. N., Vagin, A. A., Lebedev, A., Wilson, K. S. & Dodson, E. J. (1999). Efficient anisotropic refinement of macromolecular structures using FFT. *Acta Crystallogr., Sect. D: Biol. Crystallogr.* **55**, 247-255.

60. Davis, I. W., Leaver-Fay, A., Chen, V. B., Block, J. N., Kapral, G. J., Wang, X., Murray, L. W., Arendall III, W. B., Snoeyink, J., Richardson, J. S. & Richardson, D. C. (2007). MolProbity: all-atom contacts and structure validation for proteins and nucleic acids. *Nucl. Acids Res.* 35, W375-W383.

61. DeLano, W. L. (2004). The *PyMOL* Molecular Graphics System. San Carlos, CA: DeLano Scientific LLC.

62. Baker, N. A., Sept, D., Joseph, S., Holst, M. J. & McCammon, J. A. (2001). Electrostatics of nanosystems: application to microtubules and the ribosome. *Proc. Natl. Acad. Sci. USA* **98**, 10037-10041.

63. Larkin, M. A., Blackshields, G., Brown, N. P., Chenna, R., McGettigan, P. A., McWilliam, H., Valentin, F., Wallace, I. M., Wilm, A., Lopez, R., Thompson, J. D., Gibson, T. J. & Higgins, D. G. (2007). Clustal W and Clustal X version 2.0. *Bioinformatics* **23**, 2947-2948.

64. Kleywegt, G. J. & Jones, T. A. (1997). Detecting folding motifs and similarities in protein structures. *Methods Enzymol.* **277**, 525-545.

Acknowledgements

This work has been performed under the approval of the Photon Factory Program Advisory Committee (Proposal No. 2007G585). It was supported by grants-in-aid for scientific research on priority areas "Structures of Biological Macromolecular Assemblies" (to Z.-Y.W.) and Grants-in-Aid for Scientific Research (C) (No. 21570168) (to H.O.) from the Ministry of Education, Culture, Sports, Science and Technology of Japan. We wish thank the beamline staff for their help in data collection

Figure legends

Fig. 1

Biochemical analyses.

(a) Redox titration. Absorption changes at 551 nm were plotted against solution voltage. The midpoint redox potential ($E_{m,7}$) was calculated to be +188 mV.

(b) SEC-MALS analysis. The continuous line indicates the UV absorption intensity at 280 nm, and the dots represent molecular mass.

Fig. 2

The crystal structure.

(a) Two C-cyt c_z chains in the asymmetric unit. The heme groups are shown as sticks. The positions of α-helices (α1-α4) and N- and C-termini are indicated in chain A.

(b) Close-up view of the heme group in chain A. The final $2F_o$-F_c electron density map is shown as a blue mesh contoured at the 2.0 σ level, and the heme group and the coordinating residues of the heme are shown as a stick model.

(c) Contact between chains A and B*. The heme groups are shown as sticks. The positions of the N-termini are indicated in both chains.

(d) Close-up view of the interface between chains A and B*. Protein moieties, the heme groups, and PEG molecules are shown as a surface representation, a space-filling model, and a stick model, respectively. Aromatic residues (Phe, Trp and Tyr) and hydrophobic residues (Ala, Cys, Gly, Ile, Leu, Met, Pro and Val) are shown in green and

light green, respectively.

Fig. 3

Sequence alignment of cytochrome proteins.

Cyt c_z homologues of green sulfur bacteria (GSB cyt-c_z), the heme binding subunit of sulfite-oxidizing molybdoenzyme (SorB), cytochrome c_{551} (cyt-c_{551}), and cytochrome c_6 (cyt-c_6) were aligned by *CLUSTALW*[63] with some manual modifications. The secondary structure of C-cyt c_z and the positions of α-helices of cytochrome c_6 [Protein Data Bank (PDB) code 1CTJ][26] are shown above and below the sequence alignment, respectively. Fully conserved and conserved residues are shown as red and orange characters, respectively. The residues involved in hydrogen bonds to heme propionates in C-cyt c_z are shown as blue characters. The region containing high content of proline and alanine residues is indicated with a gray box. The residues indicated in Figure 7d are in pink boxes. C.tep indicates *C. tepidum*; C.lim, *C. limicola* DSM 245; P.vib, *Prosthecochloris vibrioformis*; C.fer, *Chlorobium ferrooxidans* DSM 13031; P.pha, *Pelodictyon phaeoclathratiforme* BU-1; S.nov, *Starkeya novella*; X.aut, *Xanthobacter autotrophicus* Py2; N.win, *Nitrobacter winogradskyi* Nb-255; B.jap, *Bradyrhizobium japonicum* USDA 110; M.sp, *Methylobacterium sp*. 4-46; P.aer, *P. aeruginosa*; P.stu, *Pseudomonas stuzeri*; A.vin, *Azotobacter vinelandii*; D.aro, *Dechloromonas aromatica* RCB; L.sp, *Limnobacter sp*. MED105; M.bra, *M. braunii*; S.obl, *S. obliquus*; C.rei, *Chlamydomonas reinhardtii*; S.sp, *Synechocystis sp*. PCC6803; and P.yez, *Porphyra yezoensis*.

Fig. 4

Structural resemblances between C-cyt c_z and SorB.

(a) Superposition of C-cyt c_z (orange) with SorB from *S. novella* (green, PDB code 2BLF). Superposition of the two structures with *LSQMAN*[64] shows that the root-mean-square distance is 1.22 Å for 57 C^{α} atoms. The heme groups and heme coordinating residues are shown as stick models. Numbers 1-4 show the positions of α-helices (α1-α4) in C-cyt c_z.

(b) Close-up view of the heme groups in (a). Polypeptide chains are shown as a tube model.

Figure 5

Differences between C-cyt c_z and cytochrome c_{551} or c_6.

(a) Superposition of the heme tetrapyrrole ring of C-cyt c_z (orange) and that of cytochrome c_{551} from *P. aeruginosa* (pink, PDB code 451C). The heme groups and heme coordinating residues are shown as stick models.

(b) Close-up view of the heme groups in (a). Polypeptide chains are shown as a tube model. Positions of the pyrrole rings I-IV are indicated. View from the histidine (left) or methionine (right) side of the heme plane.

(c) Superposition of the heme tetrapyrrole ring of C-cyt c_z (orange) and that of cytochrome c_6 from *M. braunii* (cyan, PDB code 1CTJ). The heme groups and heme coordinating residues are shown as stick models.

(d) Close-up view of the heme groups in (c). Polypeptide chains are shown as a tube model. View from the histidine (left) or methionine (right) side of the heme plane.

Figure 6

Heme environment.

(a) A water molecule in the heme binding pocket in chain A. Both polypeptide chain and the heme group are depicted by stick representation, and the water molecule (Wat602) is shown as a red sphere. Positions of Cys155, His156 and the pyrrole rings I-IV are indicated.

(b) Comparison of C-cyt c_z chain A (orange) and cytochrome *c* from *Saccharomyces cerevisiae* (violet, PDB code 2YCC). Water molecules and tyrosine residues near the heme propionates are depicted in sphere representation and stick representation, respectively. The major conformation is shown for the ring III propionate of chain A.

(c) Comparison of chain A (orange) and chain B (light blue). Amino acid residues and water molecules involved in hydrogen bonds via the heme propionates are shown as sticks and spheres, respectively. The major conformations are shown for Arg181 and the ring III propionate of chain A.

Figure 7

Surface properties.

(a) Surface-exposed heme group of C-cyt c_z. The heme group and the oxygen atoms of the heme propionates are shown in orange and red, respectively.

(b) Surface-exposed heme group of cytochrome c_6 from *M. braunii*. The heme group and the oxygen atoms of the heme propionate are shown in orange and red, respectively.

(c) A surface representation of C-cyt c_z colored according to electrostatic potential from -5 k_BT (red) to +5 k_BT (blue). View from the side of the surface-exposed pyrrole ring II edge.

(d) Sphere representations of C-cyt c_z. View from the same orientation as in (c). Arg151, Lys154, Lys180 and Arg181 are shown in blue. Asp192, Asp193 and Asp194 are shown in red. Phe185, Pro186 and Gly187 are colored green. The heme group is shown in yellow.

Table 1. Data collection, phasing and refinement statistics

	Fe-SAD	High resolution
Diffraction data		
Space group	$I4_1$	$I4_1$
Cell constants (Å)	$a = b = 74.5$, c = 111.3	$a = b = 74.6$, $c = 111.2$
Wavelength (Å)	1.7365	1.0000
Resolution (Å)	30-2.0 (2.07-2.00)	50-1.3 (1.32-1.30)
Unique reflections	19,890	73,534
Redundancy	22.5 (9.8)	7.7 (3.9)
R_{merge} (%)[a]	6.9 (22.7)	4.8 (19.8)
$I/\sigma(I)$	63.2 (5.4)	71.5 (4.4)
Completeness (%)	96.9 (85.3)	98.4 (94.8)
SAD phasing		
Resolution (Å)	30-2.0	
Overall FOM[b]	0.500/0.821	
Refinement		
Resolution (Å)		50-1.3
R_{work} (%)[c]		13.9
R_{free} (%)[c]		15.5

No. of protein atoms[d]		1240
No. of heme atoms[d]		91
No. of solvent atoms		320
Average *B* factor (Å^2)		25.9
Root-mean-square		
Bonds (Å)		0.011
Angles (º)		1.36
Ramachandran plot (%)[e]		99.4/0.6/0

Values in parentheses represent the highest resolution shell.

[a]$R_{merge} = \sum_{hkl}\sum_i |I_{hkl,i} - \langle I_{hkl}\rangle|/\sum_{hkl}\sum_i I_{hkl}$, where I_{hkl} is the ith measured diffraction intensity, and $\langle I_{hkl}\rangle$ is the average of the intensity. Bijvoet pairs of the data were kept separate but were scaled simultaneously, and R_{merge} values were calculated with the Bijvoet pairs merged.

[b]FOM (figure of merit) = $\Sigma P(\alpha)e^{i\alpha} / \Sigma P(\alpha)$, where α is the phase and $P(\alpha)$ is the phase probability. Before/after density modification.

[c]$R = \sum| |F_o| - |F_c| |/\sum|F_o|$.

[d]Including the atoms of residues or propionate group with double conformation.

[e]Favored/allowed/disallowed regions.

(a)

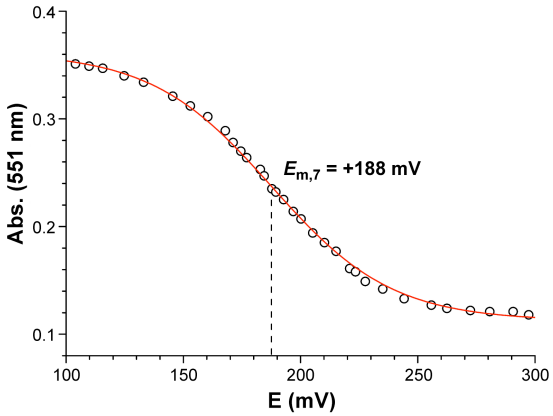

(b)

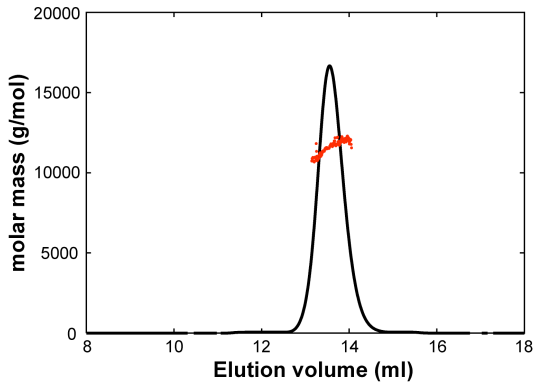

Fig. 1, Hirano *et al*.

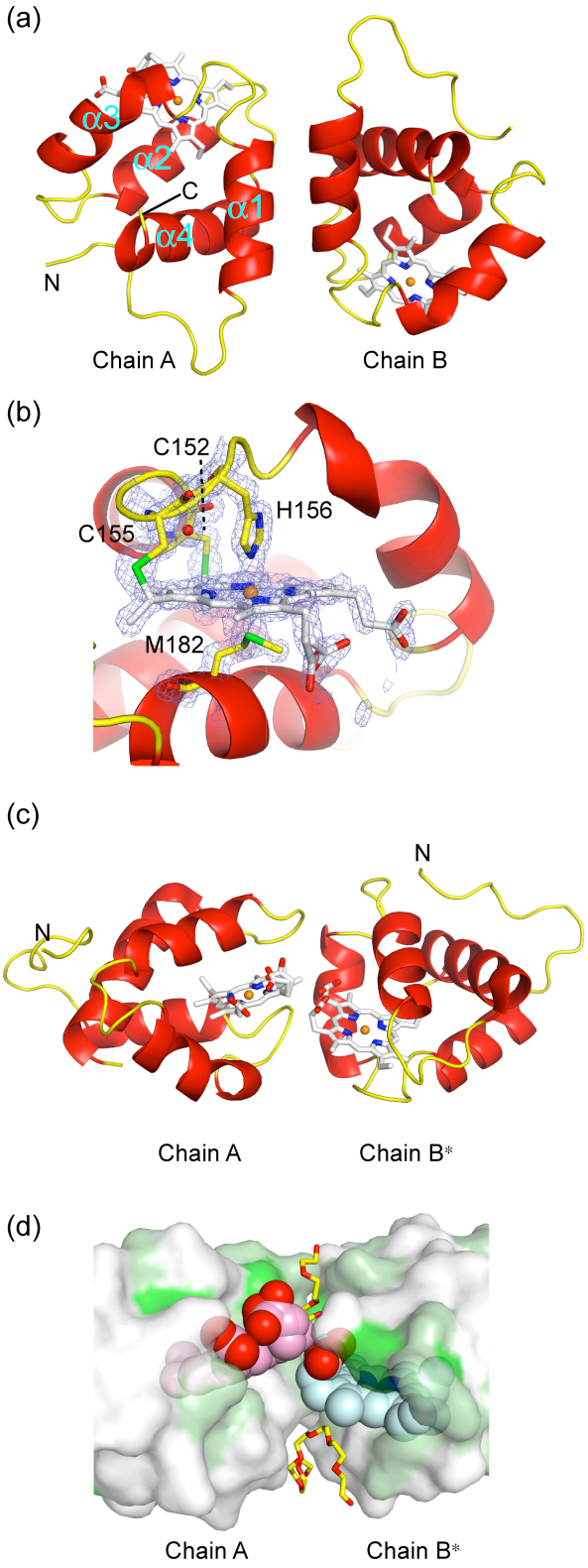

Fig. 2, Hirano *et al*

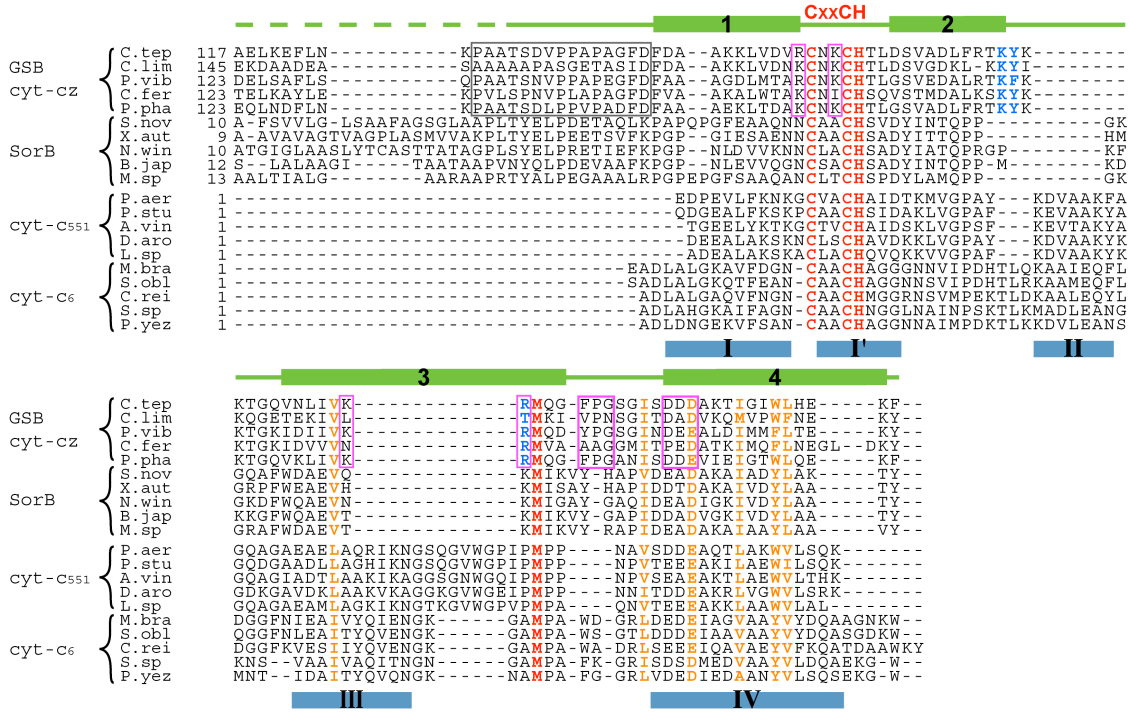

Fig. 3, Hirano *et al*.

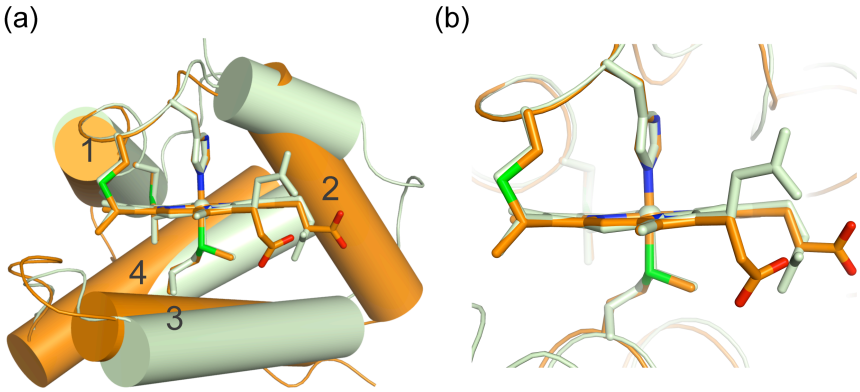

Fig. 4, Hirano *et al*.

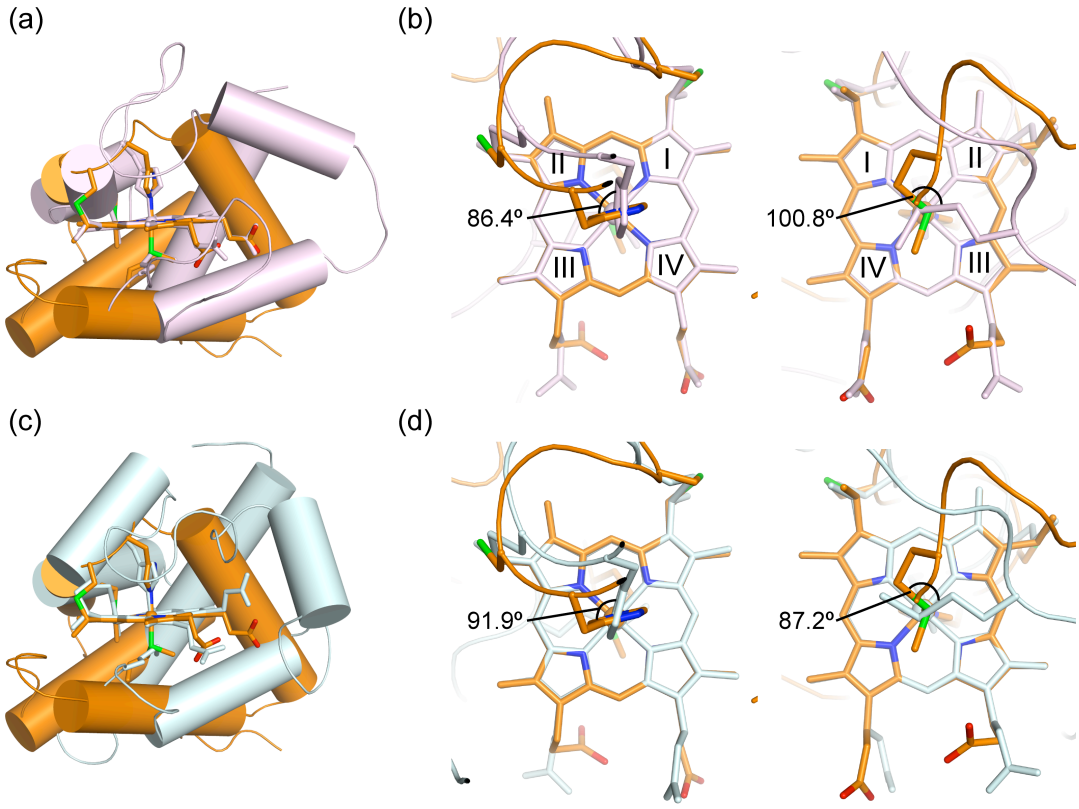

Fig. 5, Hirano *et al*.

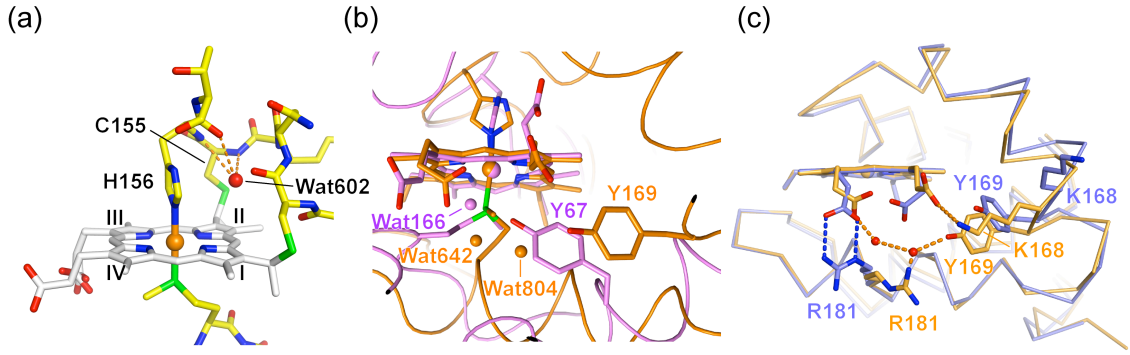

Fig. 6, Hirano *et al*.

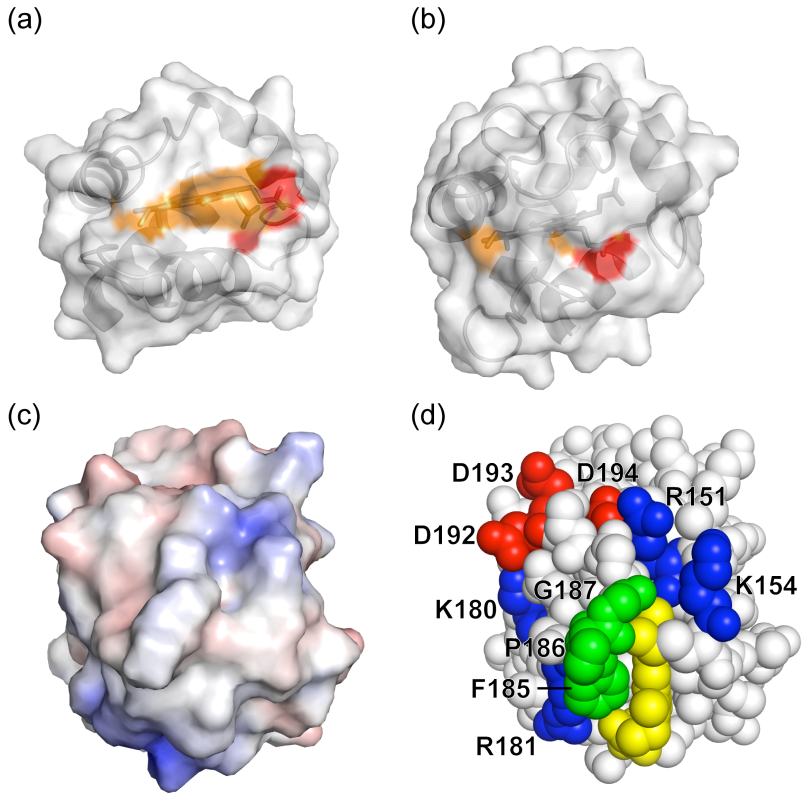

Fig. 7, Hirano *et al*.